Chemical Science

ROYAL SOCIETY OF CHEMISTRY

EDGE ARTICLE

View Article Online
View Journal | View Issue

Cite this: *Chem. Sci.*, 2024, **15**, 9104

All publication charges for this article have been paid for by the Royal Society of Chemistry

Highly acidic *N*-triflylphosphoramides as chiral Brønsted acid catalysts: the effect of weak hydrogen bonds and multiple acceptors on complex structures and aggregation†

Markus Hecht,[a] Philipp Dullinger,[b] Wagner Silva,[a] Dominik Horinek[b] and Ruth M. Gschwind*[a]

Received 22nd March 2024
Accepted 22nd April 2024

DOI: 10.1039/d4sc01939c

rsc.li/chemical-science

N-Triflylphosphoramides (NTPAs) represent an important catalyst class in asymmetric catalysis due to their multiple hydrogen bond acceptor sites and acidity, which is increased by several orders of magnitude compared to conventional chiral phosphoric acids (CPAs). Thus, NTPAs allow for several challenging transformations, which are not accessible with CPAs. However, detailed evidence on their hydrogen bonding situation, complex structures and aggregation is still lacking. Therefore, this study covers the hydrogen bonding behavior and structural features of binary NTPA/imine complexes compared to their CPA counterparts. Deviating from the single-well potential hydrogen bonds commonly observed in CPA/imine complexes, the NTPA/imine complexes exhibit a tautomeric equilibrium between two proton positions. Low-temperature NMR at 180 K supported by computer simulations indicates a OHN hydrogen bond between the phosphoramide oxygen and the imine, instead of the mostly proposed NHN H-bond. Furthermore, this study finds no evidence for the existence of dimeric NTPA/NTPA/imine complexes as previously suggested for CPA systems, both synthetically and through NMR studies.

Introduction

Building molecules with high levels of stereoselectivity and under mild reaction conditions is a major challenge in organic chemistry. Among the metal-free classes of catalysts, chiral Brønsted acids have found widespread applications.[1–3] In particular, 1,1′-Bi-2-naphthol (BINOL)-derived chiral phosphoric acids (CPAs) constitute a class of highly enantioselective catalysts available for asymmetric transformations, including Mannich-reactions, transfer hydrogenations, Strecker reactions, and many others.[1,4–7] Within the vast variety of reactions, nucleophilic additions to imines developed into the central mechanistic model system for CPAs as Brønsted acid catalysts.[8,9] Extensive NMR studies in binary CPA and *N*-arylimine complexes have been conducted previously, which proved the formation of hydrogen bond assisted ion pairs in these CPA/substrate complexes (Fig. 1A), supported by a network of CH–π and π–π interactions.[10–12] For the CPA/imine complexes, four core structures with strong POHN hydrogen bonds were observed experimentally.[11] Besides spectroscopic and experimental investigations, machine learning approaches have been key to a deeper understanding of reactivity and stereoselectivity in CPA-catalyzed reactions.[13,14] Goodman *et al.* linked the stereoselectivity to the steric properties of the 3,3′-substituents and developed a model for predicting suitable CPAs based on reactant structures.[15,16] Furthermore, Sigman *et al.* developed a data-driven prediction model to clarify the impact of various parameters on the stereoselectivity.[17–19]

However, the investigated classical chiral phosphoric acid catalysts are still limited to reactive substrates.[2] For this purpose, the groups of List and Yamamoto reported the synthesis of other highly acidic catalysts such as disulfonimides (DSIs),[20] imidodiphosphorimidates (IDPis)[21] or *N*-triflylphosphoramides (NTPAs).[22] These catalysts vary significantly from CPAs due to their increased acidity, chiral microenvironment, and the presence of multiple hydrogen bond acceptor sites, potentially enabling both OHN and NHN hydrogen bonds.[23] For DSIs detailed investigations were conducted by our group revealing the existence of binary DSI/imine complex structures with hydrogen bonds to both acceptors, the nitrogen and the oxygen of the DSI.[24,25] Furthermore, IDPi-catalyzed transformations were closely investigated by the group of List in an attempt to locate and characterize ionic or covalent species.[26,27] However, the structure and hydrogen bond situation of NTPAs has to the best of our knowledge not been intensively studied yet. Several challenging transformations

[a]*Institut für Organische Chemie, Universität Regensburg, D-93053, Regensburg, Germany. E-mail: ruth.gschwind@chemie.uni-regensburg.de*

[b]*Institute of Physical and Theoretical Chemistry, University of Regensburg, D-93053, Germany*

† Electronic supplementary information (ESI) available. See DOI: https://doi.org/10.1039/d4sc01939c

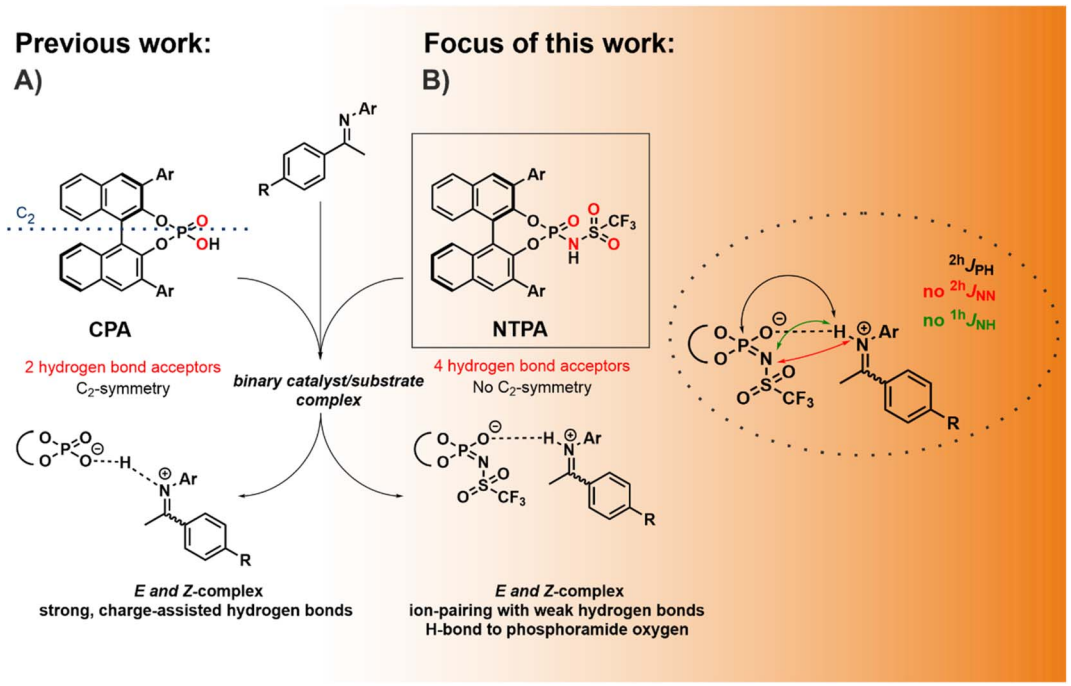

Fig. 1 (A) Previously binary complexes between CPAs and imines have been studied proving the formation of strong, charge-assisted hydrogen bonds. For the CPA/imine complexes, two different orientations of each imine isomer (*E* and *Z*) inside the binary complex were detected. (B) The focus of this work was a hydrogen bond and a structural analysis of NTPA/imine complexes addressing the influence of increased acidity of the catalyst, multiple hydrogen bond acceptors and the missing C_2 symmetry.

such as cycloadditions or addition reactions to imines which are not suitable with CPAs could be realized with NTPAs.[23,28,29] Exemplarily, the group of Yamamoto reported an asymmetric Mukaiyama–Mannich reaction, in which less reactive aldimines, without an *N*-(2-hydroxyphenyl) moiety, are activated by NTPA.[30] Subsequently, the question arises how the use of a stronger Brønsted acid such as NTPA influences the structure of the reaction intermediates and the hydrogen bond strength.[31] Furthermore, the incorporation of a *N*-trifluoromethanesulfonyl group into the CPA system breaks the C_2-symmetry of the catalyst and introduces multiple hydrogen bond acceptors (Fig. 1B). Hence, there is the question which of the several hydrogen bond acceptors is included in the resulting hydrogen bond. So far, Yamamoto *et al.* and other groups suggested that the negative charge is located at the nitrogen and consequently a hydrogen bond exists between the nitrogen of the NTPA catalyst and the substrate.[30,32–34] However, Yoon *et al.* isolated a substrate-acid complex indicating a hydrogen bond between a protonated imidazolium and the phosphoramide oxygen of the NTPA catalyst *via* X-ray crystallography.[35] Nevertheless, crystal structures do not always align with intermediates observed in solution.[36] Moreover, it is also possible that the catalyst forms two hydrogen bond with one substrate, leading to a bifunctional activation mode.[23] Therefore, the question remains what kind of H-bonding is active in NTPAs in solution. Low-temperature NMR spectroscopy at 180 K was proven to be an excellent tool to investigate the occurring intermediates as well as potential hydrogen bonds as sensitive experimental indicator for the binding situation within the binary complexes.[10,12]

Therefore, binary complexes of a NTPA catalyst with 11 different *N*-arylimines were investigated by low-temperature NMR. First, an in-depth analysis of the hydrogen bond situation in these binary NTPA/imine complexes was performed. The hydrogen bond was characterized by analyzing ^{1}H and ^{15}N chemical shifts in a Steiner–Limbach correlation and compared with the corresponding CPA/imine complexes.[37–39] Second, various two-dimensional NMR-techniques were applied at 180 K for a chemical shift assignment of the NTPA/imine systems. Based on the assignment, characteristic NOE cross signals between the catalyst and substrate were analyzed. Structures for the binary complexes based on NOE cross signals were supported by molecular dynamics (MD)-simulations. In particular, the effect of the increased number of hydrogen bond acceptors of the NTPA compared to the CPA is addressed. Finally, the NTPA catalyst was examined for its potential involvement in a dimeric reaction pathway in the Mukaiyama–Mannich reaction.

Results and discussion

Model system

In order to compare the hydrogen bonding in binary NTPA/imine complexes with the previously investigated CPA/imine complexes,[10–12] a comprehensive H-bond analysis was conducted. As catalyst we selected the commercially available NTPA **1** (Fig. 2a), which provides the opportunity for ^{19}F NMR

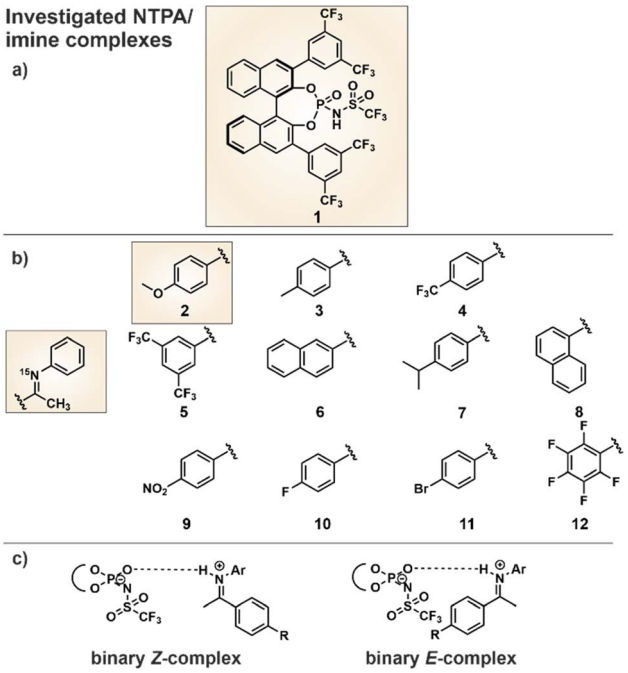

Fig. 2 (a) NTPA catalyst **1** was selected due to its 3,3′-substituents, which provide the opportunity for ^{19}F NMR measurements. (b) Structures of the imines **2–12** for the hydrogen bond analysis to cover a broad basicity range. Imine **2** was investigated in detail with NTPA **1** to gain structural insights into the binary NTPA/imine complexes. (c) The focus of this work was the NMR-spectroscopic investigation of the binary NTPA/imine complexes to clarify which of the several hydrogen bond acceptors is included in the weak hydrogen bond. The imine exists either as *E*- or *Z*-isomer.

investigations, and eleven imines **2–12** (Fig. 2b) with different electronic and steric properties. ^{15}N labeling of the imines allowed the access to the ^{15}N chemical shifts which were necessary for the determination of the hydrogen bond strength. Whereas imines **2–12** were used to cover a broad range of basicities for a H-bond analysis using the Steiner–Limbach curve, the methoxy-substituted *N*-arylimine **2** was chosen for structural investigations due to the reduced chemical shift overlap in the binary complex. Furthermore, ^{15}N labeling of NTPA **1** enabled deeper insights into a catalytic system with multiple hydrogen bond acceptors and clarification which of the hydrogen bond acceptors is included in the resulting hydrogen bond. Both, intense NOE cross peaks between imine **2** and the BINOL backbone of the NTPA as well as computer simulations were used for the structure elucidation. Finally, the NTPA **1** was examined in an enantioselective Mukaiyama–Mannich reaction to address possible reaction intermediates.[30] For NMR measurements CD_2Cl_2 was chosen as solvent, since it provides the best chemical shift dispersion and smallest line widths. All NMR spectra were recorded at 180 K to reach the slow exchange regime of the hydrogen-bonded protons (see ESI Fig. S1–S11 and S12–S14†).

Hydrogen bond analysis

The use of a Brønsted acid with a stronger external acidity such as NTPA **1** raised the question of whether binary complexes show similar hydrogen bonds to those present in the CPA/imine complexes or whether pure ion pairs without hydrogen bond contributions are formed. In general, the position of the proton within a hydrogen bond hinges on both the acidity of the hydrogen bond donor and the basicity of the hydrogen bond acceptor. The strongest hydrogen bonds are formed with the proton shifted towards the center of the hydrogen bond. With increasing acidity of the H-bond donor a hydrogen bond assisted ion-pair is formed. Finally, also a pure ion pair without hydrogen bonding can be generated by shifting the proton completely to the acceptor. The amount of proton transfer between CPA and imine was previously interpreted by the analysis of different binary CPA/imine complexes regarding ^{1}H and ^{15}N chemical shifts as well as $^{1h}J_{NH}$ coupling constants in a Steiner–Limbach correlation.[10,12,38] The correlation was developed by Limbach and Denisov in their studies of OHN hydrogen bonds in pyridine acid complexes.[37–39] Notably, our recent studies have demonstrated that this correlation is also applicable to the POHN hydrogen bonds in CPA/imine complexes.[10,12] For CPA/imine complexes, the data points derived from the hydrogen bond proton and the ^{15}N chemical shift of the hydrogen bond acceptor revealed a parabolic dependency between these two chemical shifts (Fig. 3 orange points). This suggests the existence of a single-well hydrogen bond, where the maximum of the parabolic correlation curve represents the formation of the strongest hydrogen bond.[38] In general, the calculated parabolic correlation curve is valid only

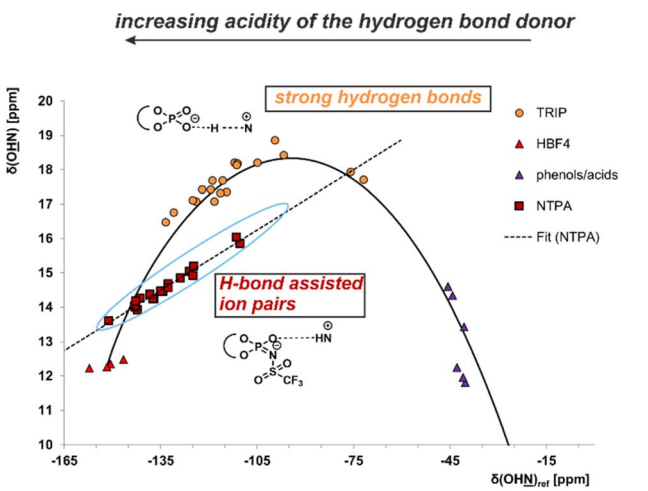

Fig. 3 Plot of $\delta(OH\underline{N})_{ref}$ against $\delta(O\underline{H}N)$ for various binary NTPA **1**/imine and CPA/imine complexes. The ^{15}N chemical shifts are referenced by $\delta(OH\underline{N})_{ref} = \delta(OH\underline{N})_{obs} - 340.8$ ppm. 340.8 ppm is the chemical shift of the free imine showing the strongest hydrogen bond in the previous work. Data points of phenols/carboxylic acids, tetrafluoroboric acid and the CPA TRIP are from previous studies (see ESI†). Binary *E*- and *Z*-complexes of NTPA **1** and imines **2–12** are depicted in red rectangles and show a deviation from the correlation curve. This is an indication for a double-well potential, which means the proton is either located at the proton acceptor or donor.

if the H-bond proton always moves in a single-well potential. When an equilibrium between two proton positions exists, indicating a double-well potential, the correlation between the two chemical shifts results in a straight line.[38] In Fig. 3, the Steiner Limbach plot of NTPA **1** is compared with that of the CPA TRIP, which is known to provide extremely strong hydrogen bonds. To cover a broad basicity range, binary complexes of NTPA **1** and TRIP with the imines **2–12** from Fig. 2 were employed.

Whereas the CPA/imine systems show chemical shifts for the hydrogen bond proton above 16 ppm and follow a parabolic curve revealing very strong hydrogen bonds (Fig. 3), the NTPA/imine *E*- and *Z*-complexes exhibit high field shifts for both ^{1}H and ^{15}N (for ^{1}H and ^{15}N spectra see ESI Fig. S1–S11†). As a result, these complexes were positioned far down on the left side of the Steiner–Limbach curve close to the almost pure ion pair with HBF_4. The position of the NTPA complexes showed that the proton within the hydrogen bond is significantly shifted toward the imine nitrogen suggesting weak or no hydrogen bonds. However, upon closer examination of the Steiner–Limbach curve, there's another significant difference between the CPA/imine complexes and the current NTPA/imine complexes. In contrast to the CPA systems, which aligned perfectly with the parabolic Steiner–Limbach correlation curve, the data points of the NTPA systems formed a straight line, deviating from the parabolic dependency.

This was the first time we observed such a trend within our catalyst systems, and it can be interpreted as explained above: the parabolic correlation curve is valid only for strong H-bond and not for a proton-transfer equilibrium between two tautomeric forms.[37,40] Therefore, the deviation of NTPA **1**/imine complexes from the parabolic ^{1}H/^{15}N chemical shift correlation curve is an indication for a double-well potential in these complexes.[37,40] This means, the proton is either located at the nitrogen of the imine or at the nitrogen/oxygen of the NTPA catalyst and upon variation of the imine basicity only the relative populations of the two positions are changed and not the hydrogen bond itself, which explains the linear correlation using the different imines. Indeed, upon examination of the $^{1h}J_{NH}$ coupling constants of the binary NTPA **1**/imine complexes, coupling constants of $^{1h}J_{NH} \sim 87$–91 Hz are detected, which are larger than for all CPA/imine complexes ($^{1h}J_{NH}$ between 82 and 86 Hz).[12] $^{1h}J_{NH}$ coupling constants are a fundamental factor for the binding strengths between proton and nitrogen of the imine. The observed $^{1h}J_{NH}$ coupling constants for the NTPA **1**/imine complexes differ only about 2–5 Hz from the completely protonated HBF_4/imine complexes. Again, this suggests very weak hydrogen bonds and a tautomeric equilibrium between two proton positions.

Structure elucidation and hydrogen bond position

To corroborate the double-well potential and to distinguish between hydrogen-bond assisted ion pairs and pure ion pairs, the scalar couplings within and through the hydrogen bonds were investigated beyond the dominating $^{1h}J_{NH}$ to the imine nitrogen. Additionally, analyzing these hydrogen bond scalar couplings could provide insights into the question which of the multiple hydrogen bond acceptors is involved in the potential hydrogen bond. However, compared to strong single-well potential hydrogen bonds a magnetization transfer through weak hydrogen bonds is typically quite challenging. Nonetheless, in order to clarify whether a scalar coupling can be detected in the hydrogen bond, we conducted 2D ^{1}H,^{31}P HMBC experiments as well as modified 1D ^{1}H,^{31}P HMBC experiments as developed by Löhr *et al.* (for details see ESI Fig. S14†).[41,42] Originally these pulse sequences were applied for the detection of scalar couplings across NH···OP and OH···OP hydrogen bonds in flavoproteins.[41] Our group also employed the modified ^{1}H,^{31}P HMBC experiments for the detection of $^{2h}J_{PH}$ scalar coupling in CPA/imine complexes.[11]

As the binary complex between NTPA **1** and imine **2** produced spectra with good signal dispersion in the hydrogen

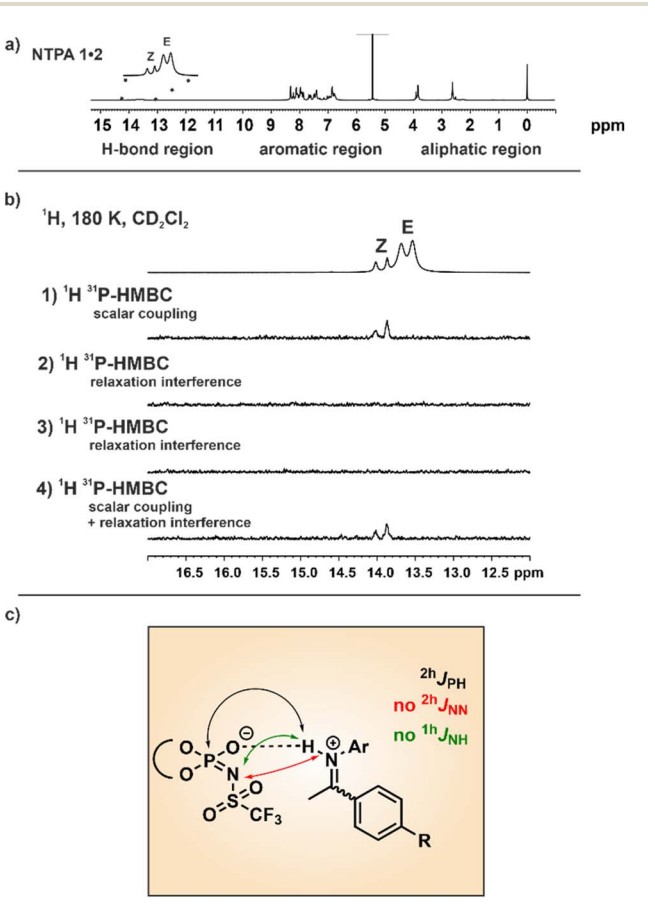

Fig. 4 (a) ^{1}H NMR spectra of the binary complexes between NTPA **1** and imine **2** at 180 K (600 MHz). Generally, the ^{1}H NMR spectra can be divided into an H-bond region, an aromatic region, and an aliphatic region. (b) ^{1}H,^{31}P HMBC H-bond section of the NTPA **1**/imine **2** complex at 180 K and 600 MHz in CD_2Cl_2. (1) Polarization transfer is mediated only by scalar coupling (2) and (3) polarization transfer is mediated by ^{1}H-CSA and ^{1}H,^{31}P-DD cross relaxation. (4) Polarization transfer is mediated by the sum of scalar coupling and the ^{1}H-CSA and ^{1}H,^{31}P-DD cross relaxation. (c) Binary complex of NTPA **1** and imine **2**. $^{2h}J_{PH}$ coupling was detected in a ^{1}H, ^{31}P HMBC experiment, whereas neither the $^{2h}J_{NN}$ coupling nor the $^{1h}J_{NH}$ coupling could be detected in a 1D ^{15}N or 2D ^{1}H,^{15}N-HSQC spectrum.

bond region, this system was chosen for the investigations (Fig. 4a).

The results from the modified $^{1}H,^{31}P$-HMBC experiments demonstrated that scalar coupling is a decisive factor for the magnetization transfer in the NTPA **1**/*Z*-imine complex, opposed to chemical shift anisotropy (CSA) or dipole interactions (Fig. 4b). The doublet corresponding to the NTPA **1**/*Z*-imine hydrogen bond was readily apparent in the modified $^{1}H,^{31}P$-HMBC sequence only allowing magnetization transfer through scalar coupling. No signals with the modified $^{1}H,^{31}P$-HMBC sequence only allowing magnetization transfer through ^{1}H chemical shift anisotropy (^{1}H-CSA) and $^{1}H,^{31}P$ dipolar interactions (DD) cross relaxation were detected. This means, that ^{1}H-CSA and DD cross relaxation is not the main origin of the magnetization transfer but scalar coupling. Detecting these cross peaks was an unexpected achievement. From the NMR spectra we cannot differentiate, whether the origin is a real $^{2h}J_{PH}$ transfer with the proton attached to the imine nitrogen or whether it comes from the low populated PXH position of the double well potential. The detection of cross peaks exclusively in the binary *Z*-complex can be attributed to two phenomena. First, the *E*-complex is involved in an exchange with the free imine (not active for *Z*) resulting in partial decoupling and therefore missing cross peaks. This is obvious from EXSY spectra (see ESI Fig. S15 and S16†) and results in an exchange broadened line width of the hydrogen-bonded proton in the ^{1}H spectrum (half line widths *E*-complex $\sim$ 50.1 Hz, *Z*-complex $\sim$ 24.7 Hz). Secondly, the observed $^{1h}J_{NH}$ coupling constants for the NTPA **1**/imine *Z*-complexes are slightly smaller than for the binary *E*-complexes, indicating a stronger hydrogen bond and thus supporting potentially $^{2h}J_{PH}$ magnetization transfer.

To conclude, our findings thus far demonstrate the presence of a weak hydrogen bond, characterized by a tautomeric equilibrium between two proton positions, in NTPA/imine complexes with a strong preference for the protonated imine. This phenomenon differs from what was observed in previously studied CPA systems.[10,12] Nevertheless, despite demonstrating the presence of a weak hydrogen bond with the $^{1}H,^{31}P$ HMBC experiments, there was still no evidence regarding which hydrogen bond acceptor is involved in the hydrogen bond. So far, mostly the negative charge was predicted to be at the nitrogen and consequently the hydrogen bond was proposed between the nitrogen of the NTPA catalyst and the substrate.[30,32–34] However, in principle, there are four potential hydrogen bond acceptors including the phosphoramide oxygen or nitrogen, as well as the triflyl oxygens. Based on the finding of the $^{1}H,^{31}P$ HMBC experiments, we can ignore the triflyl oxygens and suggest either the phosphoramide nitrogen or oxygen as the most likely hydrogen bond acceptor. To gain further insights, ^{15}N labeling of NTPA **1** was necessary. This way, potential *trans*-hydrogen bond scalar couplings ($^{1h}J_{NH}$ and $^{2h}J_{NN}$) could be detected and therefore prove a hydrogen bond between the imine and nitrogen of the NTPA, as it was proposed previously.[30,32–34] Hence, the BINOL-based ^{15}N-labeled NTPA **1** was synthesized according to the procedure of Yamamoto *et al.*[22] Since first *trans*-hydrogen bond scalar couplings were measured between nitrogen atoms of Watson–Crick base pairs in ^{15}N-labeled RNA with large coupling scalar couplings of $^{2h}J_{NN} \approx 7$ Hz, also in the NTPA complexes strong *trans*-hydrogen bond $^{2h}J_{NN}$ scalar couplings were expected.[43]

Moreover, concerning the NTPA complexes, these scalar couplings through hydrogen bonds should serve as the most effective indicator for detecting the presence of weak hydrogen bonds to the NTPA nitrogen, considering the presence of multiple other hydrogen bond acceptors. Specifically, in case of a hydrogen bond to the NTPA nitrogen, these $^{1h}J_{NH}$ scalar coupling are expected to be larger than the $^{2h}J_{PH}$ scalar couplings already detected in the modified $^{1}H,^{31}P$-HMBC experiments. However, even with ^{15}N-labeled NTPA **1** neither the $^{2h}J_{NN}$ coupling nor the $^{1h}J_{NH}$ coupling between the acidic proton and NTPA nitrogen were detectable in a 1D ^{15}N or 2D $^{1}H,^{15}N$-HSQC spectrum (see ESI Fig. S12†) Two reasons account for this phenomenon. First, the ^{15}N signal of the free labeled NTPA is sharp (half line widths $\sim$ 3.4 Hz), while the ^{15}N signal of the NTPA in the binary complex is broadened significantly (half line widths $\sim$ 53.7 Hz, for spectra see ESI Fig. S13†). This line broadening suggests again exchange processes and therefore missing cross peaks *via* partial decoupling. These exchange processes may derive from either an exchange of the hydrogen bond proton acceptor (nitrogen and oxygen) or conformational exchange.

Secondly, nitrogen might not be the main contributor in hydrogen bonding. The expected scalar coupling for a NHN hydrogen bond is around one order of magnitude larger than for a PXH situation. Furthermore, the ^{15}N line widths of both *E*- and *Z*-complexes is only double of that of ^{31}P in the binary Z-complex. Thus, the modified $^{1}H,^{31}P$-HMBC experiments indicate that, at least for the binary *Z*-complex, cross peaks should be observable in the 2D $^{1}H,^{15}N$-HSQC spectrum as well if a hydrogen bond exists between the imine and nitrogen of the NTPA. Combining then the results of the $^{1}H,^{31}P$-HMBC and the 2D $^{1}H,^{15}N$-HSQC spectrum, the phosphoramide oxygen must be regarded as the main hydrogen bond acceptor. This contradicts previous suggestions, which proposed a hydrogen bond between the imine and nitrogen of the NTPA.[30,32–34]

To corroborate the position of the hydrogen bond, further structural investigations of the NTPA/imine complexes *via* low-temperature NMR spectroscopy and molecular dynamics (MD)-simulations were applied. In previous studies of CPA/imine complexes, we identified the presence of two different orientations for each isomer within the binary complexes, independent of the CPA and the substitution of the *N*-arylimine.[11,44] Even at 180 K, the different orientations exhibit fast exchange on the NMR time scale.[11,44] However, due to significantly weaker hydrogen bonds in the NTPA/imine complexes and the multiple hydrogen bond acceptors, additional structures compared to CPAs were expected. Still, to achieve a full structure elucidation, $^{1}H,^{1}H$–COSY, $^{1}H,^{1}H$-TOCSY, $^{1}H,^{1}H$-NOESY, $^{1}H,^{19}F$-HOESY, $^{1}H,^{13}C$-HSQC, $^{1}H,^{13}C$-HMBC, $^{1}H,^{15}N$-HMBC and $^{1}H,^{31}P$-HMBC were performed with ^{15}N-labeled imine **2** and NTPA **1** at 180 K.

Based on intense NOEs between imine **2** and the BINOL backbone of the NTPA **1** (for spectra see ESI Fig. S17–S21†), computer simulations suggest a structure motif for the binary *E*-

complex as shown in Fig. 5 top (for details see ESI†). Various structures with a hydrogen bond to the phosphoramide oxygen were obtained from classical molecular dynamics simulations: one of the main structures resembles the type I *E* (here type I E_0), another one the type II *E* (here type II E_0) of the CPA complexes. The individual species were compared to the NOE data, which allowed for the identification of type I E_0 shown in the Fig. 5 top as the most likely candidate for the experimental data. Again, the hydrogen bond was located between the phosphoramide oxygen and the nitrogen of the imine. The type I E_0 species was additionally confirmed to correspond to a density functional minimum structure (B3LYP def2-TZVP with implicit CPCM solvent – for details see ESI†). Furthermore, displacing the H-bond towards N^- revealed again the type I E_0 structure as the primary minimum (details see ESI†). This suggests an H-bond as shown in Fig. 5. These findings for the binary NTPA **1**/*E*-imine complement the hydrogen bond situation identified in the NTPA **1**/*Z*-imine complex, as confirmed by scalar coupling in a $^{1}H,^{31}P$-HMBC experiment.

For the first time, there is now evidence that in NTPA catalyzed reactions, intermediates have a strong ion-pair character supported by an extremely weak hydrogen bond between the phosphoramide oxygen and the nitrogen of the imine. This finding opposes the previously proposed activation mode for NTPA-catalyzed reactions suggesting that the negative charge and consequently the hydrogen bond exists between the nitrogen of the NTPA catalyst and the substrate.[30,32–34] Our detailed hydrogen bond analysis, as well as structural investigations *via* low-temperature NMR at 180 K supported by computer simulations suggest an ion-pair character in these binary complexes supported by a weak hydrogen bond between the phosphoramide oxygen and the nitrogen of the imine. Whereas Yoon *et al.* also isolated a substrate-acid complex indicating a hydrogen bond between a protonated imidazolium and the phosphoramide oxygen of the NTPA catalyst *via* X-ray crystallography,[35] our findings confirm this binding situation in solution. We expect that these findings aid in understanding reaction intermediates, potentially shedding light on the factors contributing to the enantioselectivity of reactions, which is essential for further catalyst development.

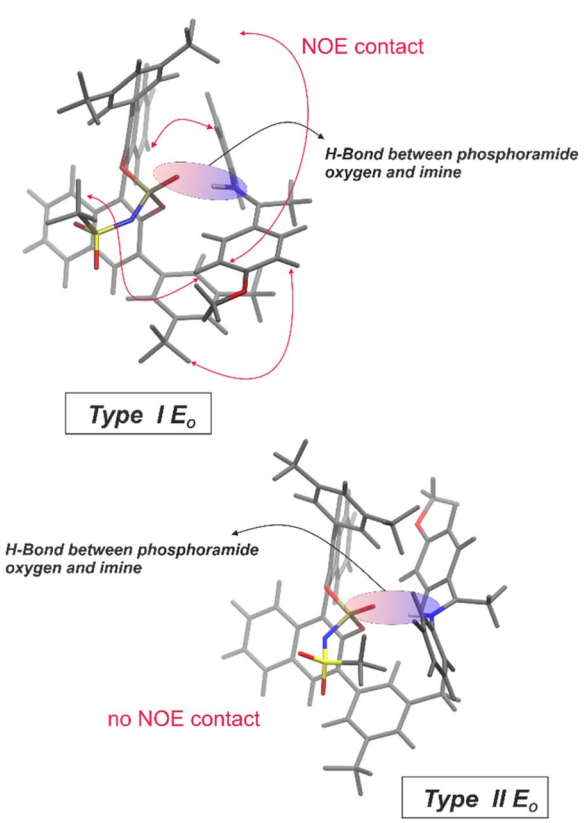

Fig. 5 Structures for the oxygen-based H-binding motif of the binary *E*-complex: inter-atomic distances obtained from molecular dynamics simulations are consistent with the intense NOE contacts for the type I E_0 structure (for details and assignment of the substructures to the NOE signals see ESI†). No NOE contacts were found for the type II E_0 structure, obtained by rotating the imine leading to the exclusion of structure motif II.

Screening for dimers in NTPA catalyzed reactions

In recent research, the transfer hydrogenation of imines with Hantzsch Ester (HE) under CPA catalysis was adopted as a model system for in-depth mechanistic studies. In our NMR studies, we observed the presence of intermediates not only involving a single catalyst molecule but also those involving two catalyst molecules.[45,46] Furthermore, Niemeyer *et al.* revealed that supramolecular linked CPAs show cooperativity effects in the transformation of quinolines.[45] This discovery raised the question, whether competing monomeric and dimeric reaction pathways may be a general feature in Brønsted acid catalysis. Lately, Franta *et al.* demonstrated that a dimeric pathway is active for a broad variety of CPAs typically used in the synthesis of chiral amines leading to opposite enantioslectivities.[47] Additonally, dimeric formation could be observed by low-temperature NMR at 180 K.

This raised the question of whether the observed phenomenon is also applicable to NTPAs, addressing the presence of a sterically demanding *N*-trifluoromethanesulfonyl group and the absence of a C_2-symmetry. Therefore, we examined NTPA **1** in an enantioselective Mukaiyama–Mannich reaction developed by the group of Yamamoto to address possible reaction intermediates (Table 1).[30] Significantly, the challenge of achieving enantioselective Mukaiyama–Mannich reactions catalyzed by chiral phosphoric acids, which previously needed a 2-hydroxyphenyl moiety on the aldimine, was solved by taking advantage of a NTPA catalyst.[30] Previously, a NTPA catalyst bearing 2,4,6-trimethyl-3,5-dinitrophenyl substituents at the 3,3′-positions enabled the reactions with excellent enantioselectivities up to 95% ee.[30]

To check, whether intermediates involving two catalyst molecules are present in the NTPA/imine complexes too, we conducted both a synthetic study and an NMR study. In this study, we once more employed NTPA **1** featuring 3,5-bis trifluoromethyl phenyl substituents at the 3,3′-positions, as in previously investigated CPA systems these substituents showed a general preference for dimerization.[47] In the synthetic part we

Table 1 NTPA **1** was examined in an enantioselective Mukaiyama–Mannich reaction developed by the group of Yamamoto to address possible dimeric intermediates. In the synthetic part we aimed to achieve an inversion of enantioselectivity by varying temperature and catalyst loading in the Mukaiyama–Mannich reaction. Contrary to our expectations of observing an inversion, we merely observed a decrease in enantioselectivity from 86% ee to 56% ee as temperature was increased

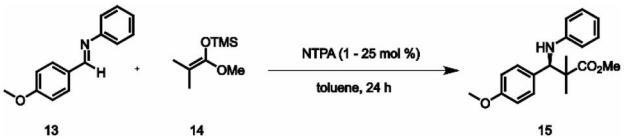

Entry	Temp. [°C]	Cat. loading [%]	ee [%]
1	r.t.	0.1	No conversion
2	r.t.	10	72
3	r.t.	25	66
4	−10	0.1	No conversion
5	−10	10	76
6	−10	25	80
7	80	1	56
8	80	10	56
9	−80	25	86

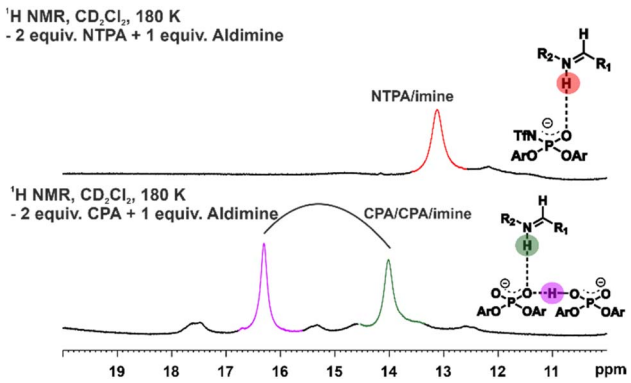

Fig. 6 Low-temperature NMR at 180 K was used to investigate the presence of dimers in a 2 : 1 ratio of catalyst to imine. In the samples with a 2 : 1 ratio of NTPA to imine, no dimeric formation was identified. However, when employing a 2 : 1 ratio with CPA to imine, dimer formation became evident in the ^{1}H NMR spectrum.

aimed to achieve an inversion of enantioselectivity by varying temperature and catalyst loading in the Mukaiyama–Mannich reaction, as it was previously seen in the transfer hydrogenation of imines under CPA catalysis.[47] During the reaction, we applied temperatures ranging from −80 °C to +80 °C. Contrary to our expectations of observing an inversion, we merely observed a decrease in enantioselectivity from 86% ee to 56% ee (Table 1). When the catalyst loadings were varied from 0.1% to 25%, only minor differences in enantioselectivity were detected. Consequently, the synthetic approach did not reveal any indication of a dimeric pathway.

Subsequently, the selection of low-temperature NMR was chosen to examine the existence of dimers. Best conditions for the study were determined to be a 2 : 1 ratio of catalyst to either quinoline or imine, as established in previous research.[45,47,48] However, no 2 : 1 NTPA/NTPA/imine dimer formation with ketimines or aldimines was observed in the ^{1}H-NMR spectrum (Fig. 6). Previously, a characteristic pattern for dimers could be identified in the hydrogen bond region of the ^{1}H-spectrum using CPAs (Fig. 6). We assume that the difference in hydrogen bond strength and steric demands of the *N*-trifluoromethanesulfonyl group is responsible for this phenomenon. Our findings suggest only the presence of the monomeric pathway for NTPA based Brønsted acid catalysis reactions.

Conclusions

The investigation into the application of NTPAs as catalysts in asymmetric catalysis has provided valuable insights into their structural behavior and reactivity. By conducting an in-depth analysis of the strength and positioning of hydrogen bonds within binary NTPA/imine complexes, distinct characteristics of NTPAs have emerged in comparison to CPAs. Notably, our study has unveiled the presence of a weak hydrogen bond between the phosphoramide oxygen and the imine, characterized by a proton-transfer equilibrium between two tautomeric forms, challenging previous assumptions regarding the activation mechanism of NTPAs. Also computer simulations support an ion-pair character in these binary complexes and predict a weak hydrogen bond between the phosphoramide oxygen and the nitrogen of the imine. Additionally, our investigation of the NTPA-catalyzed Mukaiyama–Mannich reaction revealed that the coexistence of monomeric and dimeric reaction pathways, previously observed in CPA-catalyzed reactions, does not apply to NTPAs. This difference is attributed to the unique properties of the sterically demanding *N*-trifluoromethanesulfonyl group resulting in higher acidity of the catalyst and therefore weaker hydrogen bonds. Ongoing investigations aim to further elucidate the distinctive behavior of NTPAs, facilitating their application in asymmetric catalysis.

Data availability

Necessary data is given in the ESI.† For further information ask the corresponding author.

Author contributions

M. H. and R. G. conceived and conceptualized the project. M. H. planned and performed all experiments. Analysis of all experiments was done by M. H., W. S. and R. G. All calculations were performed by P. D. and analyzed by P. D. and D. H. Visualization was done by M. H. and P. D., interpretation of results, writing and revision of the manuscript was done by all authors. R. G. and D. H. provided funding and resources.

Conflicts of interest

There are no conflicts to declare.

Acknowledgements

This project was financed by the German Science Foundation (DFG; RTG 2620) project number 426795949. P. D. thanks the German Academic Scholarship Foundation for funding.

References

1 D. Parmar, E. Sugiono, S. Raja and M. Rueping, *Chem. Rev.*, 2014, **114**, 9047.
2 T. Akiyama and K. Mori, *Chem. Rev.*, 2015, **115**, 9277.
3 M. Mahlau and B. List, *Angew. Chem., Int. Ed.*, 2013, **52**, 518.
4 J. M. M. Verkade, L. J. C. van Hemert, P. J. L. M. Quaedflieg and F. P. J. T. Rutjes, *Chem. Soc. Rev.*, 2008, **37**, 29.
5 T. Akiyama, J. Itoh, K. Yokota and K. Fuchibe, *Angew. Chem., Int. Ed.*, 2004, **43**, 1566.
6 D. Uraguchi and M. Terada, *J. Am. Chem. Soc.*, 2004, **126**, 5356.
7 M. Yamanaka, J. Itoh, K. Fuchibe and T. Akiyama, *J. Am. Chem. Soc.*, 2007, **129**, 6756.
8 S. J. Connon, *Angew. Chem., Int. Ed.*, 2006, **45**, 3909.
9 S. Hoffmann, A. M. Seayad and B. List, *Angew. Chem., Int. Ed.*, 2005, **44**, 7424.
10 N. Sorgenfrei, J. Hioe, J. Greindl, K. Rothermel, F. Morana, N. Lokesh and R. M. Gschwind, *J. Am. Chem. Soc.*, 2016, **138**, 16345.
11 J. Greindl, J. Hioe, N. Sorgenfrei, F. Morana and R. M. Gschwind, *J. Am. Chem. Soc.*, 2016, **138**, 15965.
12 K. Rothermel, M. Melikian, J. Hioe, J. Greindl, J. Gramüller, M. Žabka, N. Sorgenfrei, T. Hausler, F. Morana and R. M. Gschwind, *Chem. Sci.*, 2019, **10**, 10025.
13 L. Simón and J. M. Goodman, *J. Am. Chem. Soc.*, 2008, **130**, 8741.
14 A. F. Zahrt, J. J. Henle, B. T. Rose, Y. Wang, W. T. Darrow and S. E. Denmark, *Science*, 2019, **363**, eaau5631.
15 J. P. Reid and J. M. Goodman, *J. Am. Chem. Soc.*, 2016, **138**, 7910.
16 J. P. Reid and J. M. Goodman, *Chem.–Eur. J.*, 2017, **23**, 14248.
17 J. P. Reid and M. S. Sigman, *Nature*, 2019, **571**, 343.
18 M. Orlandi, J. A. S. Coelho, M. J. Hilton, F. D. Toste and M. S. Sigman, *J. Am. Chem. Soc.*, 2017, **139**, 6803.
19 A. J. Neel, A. Milo, M. S. Sigman and F. D. Toste, *J. Am. Chem. Soc.*, 2016, **138**, 3863.
20 P. García-García, F. Lay, P. García-García, C. Rabalakos and B. List, *Angew. Chem., Int. Ed.*, 2009, **48**, 4363.
21 P. S. J. Kaib, L. Schreyer, S. Lee, R. Properzi and B. List, *Angew. Chem., Int. Ed.*, 2016, **55**, 13200.
22 D. Nakashima and H. Yamamoto, *J. Am. Chem. Soc.*, 2006, **128**, 9626.
23 G. Caballero-García and J. M. Goodman, *Org. Biomol. Chem.*, 2021, **19**, 9565.
24 K. Rothermel, M. Žabka, J. Hioe and R. M. Gschwind, *J. Org. Chem.*, 2019, **84**, 13221.
25 M. Žabka and R. M. Gschwind, *Chem. Sci.*, 2021, **12**, 15263.
26 H. Zhou, Y. Zhou, H. Y. Bae, M. Leutzsch, Y. Li, C. K. De, G.-J. Cheng and B. List, *Nature*, 2022, **605**, 84.
27 R. Properzi, P. S. J. Kaib, M. Leutzsch, G. Pupo, R. Mitra, C. K. De, L. Song, P. R. Schreiner and B. List, *Nat. Chem.*, 2020, **12**, 1174.
28 A. Borovika and P. Nagorny, *Tetrahedron*, 2013, **69**, 5719.
29 T. Hashimoto, H. Nakatsu, K. Yamamoto and K. Maruoka, *J. Am. Chem. Soc.*, 2011, **133**, 9730.
30 F. Zhou and H. Yamamoto, *Angew. Chem., Int. Ed.*, 2016, **55**, 8970.
31 K. Kaupmees, N. Tolstoluzhsky, S. Raja, M. Rueping and I. Leito, *Angew. Chem., Int. Ed.*, 2013, **52**, 11569.
32 S. P. Bew, J. Liddle, D. L. Hughes, P. Pesce and S. M. Thurston, *Angew. Chem., Int. Ed.*, 2017, **56**, 5322.
33 P. C. Knipe and M. D. Smith, *Org. Biomol. Chem.*, 2014, **12**, 5094.
34 H.-H. Liao, A. Chatupheeraphat, C.-C. Hsiao, I. Atodiresei and M. Rueping, *Angew. Chem., Int. Ed.*, 2015, **54**, 15540.
35 E. M. Sherbrook, M. J. Genzink, B. Park, I. A. Guzei, M.-H. Baik and T. P. Yoon, *Nat. Commun.*, 2021, **12**, 5735.
36 S. O. Garbuzynskiy, B. S. Melnik, M. Y. Lobanov, A. V. Finkelstein and O. V. Galzitskaya, *Proteins*, 2005, **60**, 139.
37 S. Sharif, G. S. Denisov, M. D. Toney and H.-H. Limbach, *J. Am. Chem. Soc.*, 2007, **129**, 6313.
38 H.-H. Limbach, M. Pietrzak, S. Sharif, P. M. Tolstoy, I. G. Shenderovich, S. N. Smirnov, N. S. Golubev and G. S. Denisov, *Chem.–Eur. J.*, 2004, **10**, 5195.
39 H. Benedict, I. G. Shenderovich, O. L. Malkina, V. G. Malkin, G. S. Denisov, N. S. Golubev and H.-H. Limbach, *J. Am. Chem. Soc.*, 2000, **122**, 1979.
40 S. Sharif, G. S. Denisov, M. D. Toney and H.-H. Limbach, *J. Am. Chem. Soc.*, 2006, **128**, 3375.
41 F. Löhr, S. G. Mayhew and H. Rüterjans, *J. Am. Chem. Soc.*, 2000, **122**, 9289.
42 G. Federwisch, R. Kleinmaier, D. Drettwan and R. M. Gschwind, *J. Am. Chem. Soc.*, 2008, **130**, 16846.
43 A. J. Dingley and S. Grzesiek, *J. Am. Chem. Soc.*, 1998, **120**, 8293.
44 M. Melikian, J. Gramüller, J. Hioe, J. Greindl and R. M. Gschwind, *Chem. Sci.*, 2019, **10**, 5226.
45 D. Jansen, J. Gramüller, F. Niemeyer, T. Schaller, M. C. Letzel, S. Grimme, H. Zhu, R. M. Gschwind and J. Niemeyer, *Chem. Sci.*, 2020, **11**, 4381.
46 J. Gramüller, M. Franta and R. M. Gschwind, *J. Am. Chem. Soc.*, 2022, **144**, 19861.
47 M. Franta, J. Gramüller, P. Dullinger, S. Kaltenberger, D. Horinek and R. M. Gschwind, *Angew. Chem., Int. Ed.*, 2023, **62**, e202301183.
48 R. Mitra, H. Zhu, S. Grimme and J. Niemeyer, *Angew. Chem., Int. Ed.*, 2017, **56**, 11456.